Journal of Thermal Analysis and Calorimetry, Vol. 71 (2003) 893–903

THERMAL EFFECTS IN LOW-PRESSURE PLANE PLASMA APPARATUS FOR THIN FILMS APPLICATIONS

G. Golan[*]*, A. Axelevitch, B. Sigalov and B. Gorenstein*

Faculty of Electrical Engineering, Holon Academic Institute of Technology, Open University of Israel, P.O. Box 39328, Tel Aviv 61392, Israel

Abstract

Thermal effects in a low-pressure plane plasma discharge were obtained in a novel implementation of triode sputtering method. This plane plasma discharge is formed in a relatively low vapor pressure of 0.03–0.65 Pa. Electron beam temperature and ion beam concentration distribution, as well as their dependence on argon pressure within the plasma, were experimentally studied, using the Langmuir probe technique. The influence of an external magnetic field on the ion beam concentration, and electron beam temperature, were studied too. As a result of these studies, sputtering of various materials was done using the novel plane plasma discharge method. This method enables the deposition of homogeneous thin film coatings. Analysis is done on Cu sputtered layers with plane plasma discharge.

Keywords: plane plasma, plasma, plasma thermal analysis, sputtering

Introduction

Sputtering is one of the most widely used vacuum deposition methods in the semiconductor [1] and microelectronics industries [2]. Sputtered films have suitable adhesion and good reproducibility. In addition, sputtered thin films suffer from structural disturbances and stoichiometric deviations due to the high energy impinging particles at the substrate [3] and plasma influence on the growing film. When hot plasma comes in contact with a sample substrate in a conventional magnetron sputtering system, it negatively acts on the properties of the grown film. The substrate is negatively charged and undergoes a mechanical damage as a result of the impinging plasma ions [4]. Furthermore, this negatively charged substrate causes uncontrollable variations in the film's growth rate, thus contaminating the deposited films. Moreover, the hot plasma provides an uncontrolled heat to the growing film, thus varying its physical properties.

The main goal of our work was to develop a sputtering based method, to enable a separate control on various parameters during a deposition process and to protect the substrate from plasma influences. The second goal of this work was to reduce the

* Author for correspondence: E-mail: gady@atct.co.il

1388–6150/2003/ $ 20.00

Akadémiai Kiadó, Budapest
Kluwer Academic Publishers, Dordrecht

working pressure while sputtering. For this purpose we used an artificially supported plasma discharge. The idea behind this approach was to create a plane plasma, embedded between the sputtering target and the substrate, in order to enable the sputtered atoms to reach the substrate without collisions with gas atoms and argon ions.

Experimental

The experiments were done using a laboratory setup equipped with a standard vacuum system, providing a residual vacuum of $3 \cdot 10^{-3}$ Pa (Fig. 1). A principle arrangement of the sputtering system is shown in Fig. 2. It consists of a thermo-emissive cathode, an anode placed opposite to the cathode, and a water-cooled target holder. The cathode is made of a tungsten wire, 0.5 mm diameter, braided in a spiral shape of 5 mm, 8 turns and 20 mm long. The anode was prepared in a square tantalum sheet shape, 0.5 mm thick and 56 cm^2 surface area, located in a distance of 15 cm from the cathode. A tantalum collimating aperture was placed above the cathode to form the electron beam, directed to the anode. The target and the substrate surfaces were positioned in parallel. Both of them were perpendicular to the anode–cathode axis. All of these three electrical sources (cathode heating supply, anode supply, applied between anode and cathode, and sputtering supply, applied between the target and a special ring electrode inserted in plasma, were isolated from ground. Two external electromagnetic coils, 34 cm in diameter, made of a copper wire with 550 turns, 1 mm in diameter, were wound co-axially in the anode–cathode axis to create homogeneous magnetic field, in a plane plasma shape, between target and substrate.

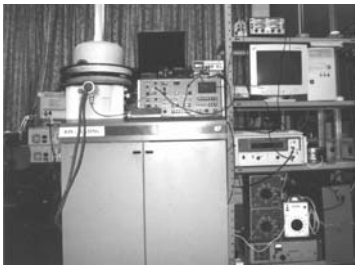

Fig. 1 An external view of the experimental sputtering machine

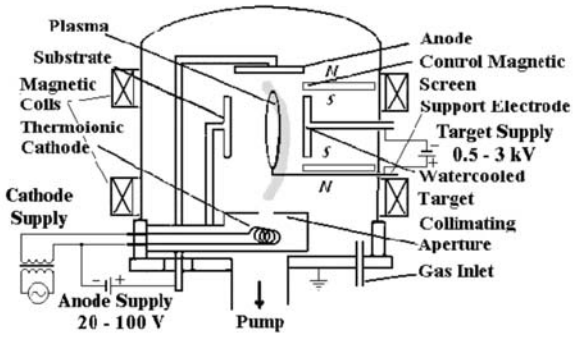

Fig. 2 The sputtering system

Plasma parameters were studied using the Langmuir probe stationary method [5]. The applied probe was made of a tungsten wire, 0.25 mm diameter, screened by a ceramic tube. The active part of the probe was 3.4 mm long. The probe area was 2.67 mm^2. The probe was placed within the plasma, and biased from –60 to +60 V, via a serial resistor R=5.7 Ω. Measurements were taken for various pressures in the vacuum chamber in various points. The distance 'a' between the probe and anode–cathode vertical axis, as shown in Fig. 3, was taken as a variable.

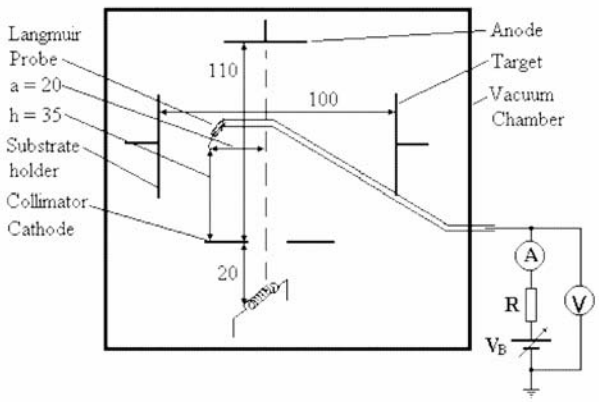

Fig. 3 Vacuum chamber geometry for the Langmuir probe measurement

Table 1 Typical parameters in a triode sputtering process

Number	Parameter	Symbol	Unit	Value
1	Residual pressure	P_{res}	Pa	$(3–4)\cdot10^{-3}$
2	Argon (work) pressure	P_{Ar}	Pa	$(7–20)\cdot10^{-2}$
3	Electromagnet current	I_h	A	2–4
4	Cathode current	I_c	A	14–16
5	Anode voltage	V_a	V	30–50
6	Sputtering voltage	V_t	V	1000–2000
7	Target current	I_t	mA	20–40
8	Substrate temperature	T_s	°C	50–300

Metal Cu plate, 50 mm in diameter, was used as a sputtering target material. The electrical properties of the deposited films were then evaluated. A standard four-point probe method was used to measure the sheet resistance of the films. The surface structure of the obtained films was studied in a computerized metallurgical microscope with optical magnification up to ×1600. Film thickness was measured on the home-made computerized micro-interferometer [6]. The glass substrates were cleaned using iso-propanol and ultra-sound bath. Temperature of the growing films while sputtering and cathode radiation heat influence on the probe placed in plasma,

were measured by a standard thermocouple K-type (Cromega–Alomega). Magnetic field strength of the external magnetic coils was measured by Digital Teslameter DTM-132 PG, using a Hall probe.

Typical parameters of the sputtering process are presented in Table 1.

Results and discussion

The magnetic field distribution inside the vacuum chamber is presented in Figs 4 and 5. Figure 4 presents the radial distribution of the magnetic field in the vacuum chamber for various coil currents. Figure 5 presents the axial distribution of the magnetic field for the external coils, measured in various coil currents. These distributions generate the magnetic field map inside the vacuum chamber. The magnetic field map is used then to estimate the magnetic field influence on charged carries moving within the plasma.

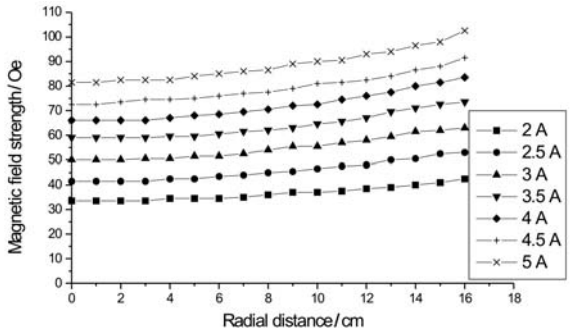

Fig. 4 Magnetic field radial distribution for various magnetic coils currents

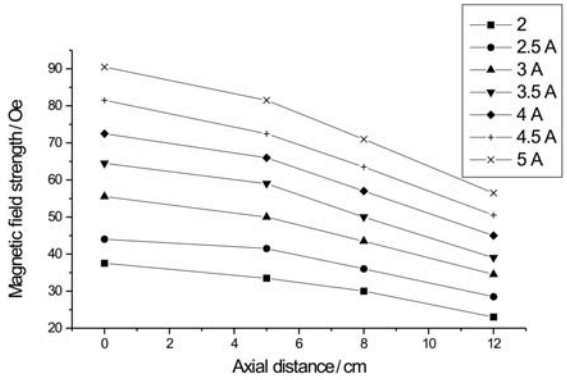

Fig. 5 Magnetic field axial distribution for various magnetic coils currents

Figure 6 illustrates a typical Langmuir probe results, measured in plane plasma. These results look much the same as typical voltage–current Langmuir characteristics

[7]. Both the floating potential V_f and the plasma potential V_P, can be precisely found in these curves. At a probe bias voltage $V_B=V_P$, the probe is at the same potential of the plasma and mainly draws current from the excess mobile carriers (electrons). This current is designated as a positive current flowing from the probe into the plasma. For V_B exceeding this value, the probe current tends to saturate at the electron saturation current. The saturation current is defined by the probe geometry. At $V_B<V_P$, electrons are repelled in accordance with the Boltzmann relationship, until at V_f the probe is sufficiently negative with respect to the plasma, so that the electron and ion currents are equal, and a measured current I=0. For $V_B<V_f$, the current is mainly ion current (negative with respect to the plasma) and tends to saturate at the ion saturation current. This current may also vary with the applied voltage and due to changes in the probe effective collection area. The value of the ion saturation current is much lower than that of the electron saturation current due to a much greater ion mass. The electron temperature may be estimated from the probe current graph at $V_f<V_b<V_P$ region in Fig. 6, using the Boltzmann distribution for electrons [8].

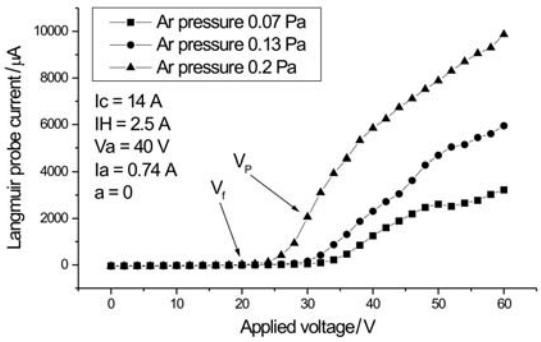

Fig. 6 Typical Langmuir probe parameters

The measurement diagram and probe construction were chosen in compliance with the experimental conditions and plasma parameters. In order to select a model for the plasma, to estimate the plasma parameters, we make interrelation between the three basic parameters: λ (the mean free path), λ_D (Debye radius), and r_p (the probe radius). The mean free path of gas molecules in a vacuum chamber can be calculated from the well known relation [9]:

$$\lambda \approx 5 \cdot 10^{-3}/p \text{ [cm]}, \quad (1)$$

where p [Torr] is the gas pressure in the vacuum chamber.

The Debye length is a typical parameter. A small deviation in the charge density from equilibrium, within this length, is relaxed or screened (in other words, is no longer felt [10]). A characteristic feature of the plasma is its ability to screen out an electrical charge. A potential disturbance within the plasma will attract particles of the opposite charge, and the cloud of charged particles provides screening to the rest of the plasma. This phenomenon is referred to as Debye screening [11]. The screening length is equal to

$$\lambda_D = \sqrt{\frac{\varepsilon_0 kT}{n_0 e^2}} \tag{2}$$

or approximately, it can be described by the following expression [2]:

$$\lambda_D \approx 743\sqrt{\frac{T_e}{n_e}[\mathrm{cm}]} \tag{3}$$

where ε_0 is the free space permittivity, k is the Boltzmann constant, e is the electron charge, n_0 is the charged particles concentration, n_e is the electrons concentration, T is the absolute gas temperature, and T_e is the electron temperature.

A layer of volume charge surrounds the probe [2]. The layer thickness is most significant for the measurement. Three typical cases can be described:

1. $\lambda >> r_p >> \lambda_D$, thin layer of volume charge;
2. $\lambda >> \lambda_D >> r_p$, collisionless thick layer of volume charge;
3. $\lambda_D >> \lambda >> r_p$, thick layer of volume charge with particle collisions.

If the pressure in the vacuum chamber does not exceed the level of 0.133 Pa, the mean free path according to Eq. (1) is equal to λ=5 cm. Weakly ionized plasma comprises of approximately 0.01% ionized particles in a volume unit [12]. The gas molecule concentration can be obtained from the known equation [13]:

$$p = n_g kT \tag{4}$$

Here n_g is the molecule concentration. Hence, the electron concentration in argon atmosphere with a pressure of 0.133 Pa, is approximately $3.21 \cdot 10^{11}$ cm^{-3}. If we assume that the electron temperature of the weakly ionized plasma is: 1–10 eV [14], then the Debye radius will be equal to λ_D=0.04–0.126 mm (from Eq. (3)).

Comparison between the parameters r_p, λ_D and λ, shows that they satisfy the first case, or: $\lambda >> r_p >> \lambda_D$, i.e. collisionless thin layer of a volume charge. This is the case of 'molecular plasma' with a Knudsen's number: $K_n = \lambda / r_p >> 1$. The thickness of the volume discharge in this case is of several Debye radices. This way we may estimate the electron temperature in plasma, using the experimental I–V characteristics of the Langmuir probe [5]:

$$T_e = \frac{e}{k}\left(\frac{\mathrm{d}V_B}{\mathrm{d}\ln J_e}\right) \tag{5}$$

Here J_e is the current density on the probe. This 'ideal' parameter ignores the 'perturbation' processes such as bombardment of the probe by high-energy electrons, emission of secondary electrons from the probe, and etching processes of the probe.

The collisionless condition allows us to use the Bohm approximation [15] to estimate the ion concentration in plasma:

$$j_{is} = en_i\sqrt{\frac{kT_e}{m_i}} \tag{6}$$

where j_{is} is the probe ion current saturation density, n_i is the ion concentration in plasma, and m_i is the argon ion mass.

This way we may use the obtained voltage–current characteristics of the Langmuir probe, as in Fig. 6, to estimate the basic plane plasma properties. For example, V_f and V_P values are marked in Figs. 6 and 7 presenting the electron temperature distribution in a plasma volume, estimated according to Eq. (5), for different gas pressures. It can be easily seen that maximum plasma temperature occurs at the axis a=0. This phenomenon is explained by the magnetic field distribution within the vacuum chamber. As shown in Fig. 4, the magnetic field is not homogeneous there, and slowly increases while drawing away from the vacuum chamber center.

The electron temperature depends on the gas pressure. It decreases with a pressure increase. It is much the same as pressure increase relates to the mean free path decrease, and as a result a decrease in electrons energy. These phenomena are illustrated in Fig. 7.

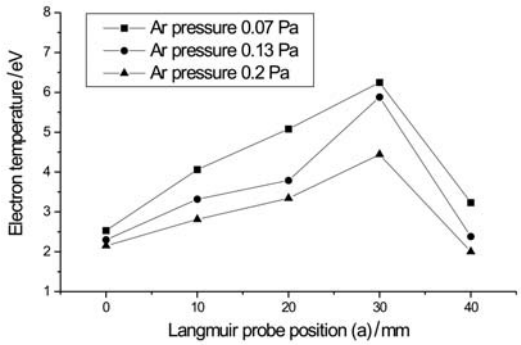

Fig. 7 Electron temperature distribution in plasma volume for various argon pressures

Ion concentration was calculated according to Eq. (6). Maximum ion concentration was obtained in a shape of a thin sheet. It should be noted that visually the plasma looks as a real thin sheet. Figure 8 presents the ion concentration distribution in the plasma volume for various gas pressures. Evidently, the ion concentration essentially depends on the gas pressure. The ion concentration increases with gas pressure increase. The ion concentration and the electron temperature, for the same gas pressure, are matched in Fig. 9. The thin wall plasma looks like slightly shifted relative to the anode–cathode vertical axis. Maximum electron temperature is shifted the same direction as well. This shift may be explained by the non-homogeneous magnetic field within the vacuum chamber. The sharp decrease in the ion concentration and electron temperature on the plasma boundaries verify our assumption of a non-influencing plasma on the substrate properties. Much the same, the plasma does not influence the cathode by increasing the substrate's temperature. The temperature of the probe, taken by a thermocouple, placed into the plasma, opposite to the cathode (a=20 mm), was studied. Heat characteristics appear in Fig. 10. It can be seen that the temperature is self-adjusted for about 15 min and not exceed 140°C. The substrate temperature does not exceed ~50°C. Therefore, substrate temperature may be chosen respectively to the specific required deposition process.

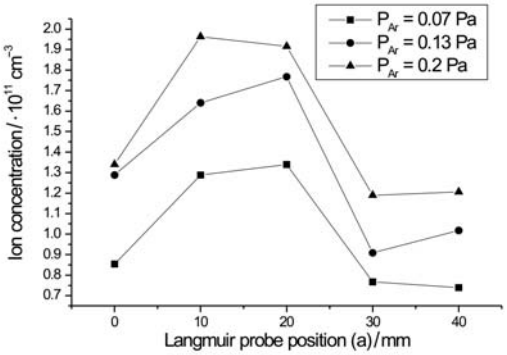

Fig. 8 Ion distribution in plasma volume for various argon pressures

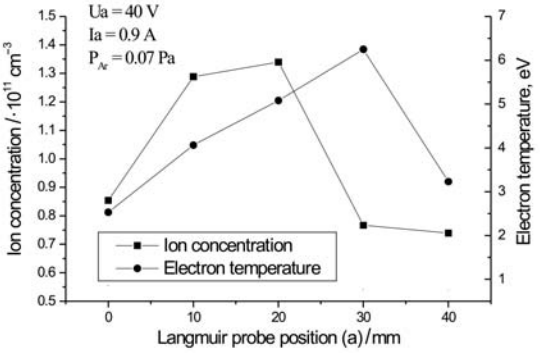

Fig. 9 Plane plasma parameters for the low pressure

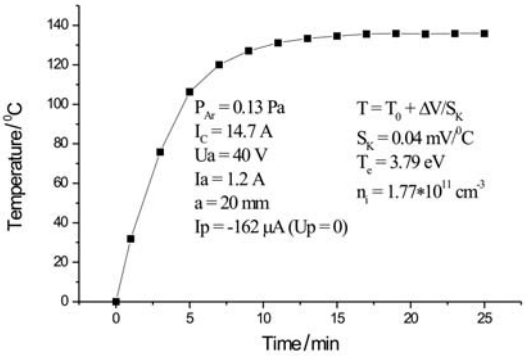

Fig. 10 Langmuir probe heat by the cathode irradiation

The plasma potential and plasma current influence are presented in Fig. 11. As shown there, the ion concentration increases with the increase in plasma potential and the electron temperature decreases.

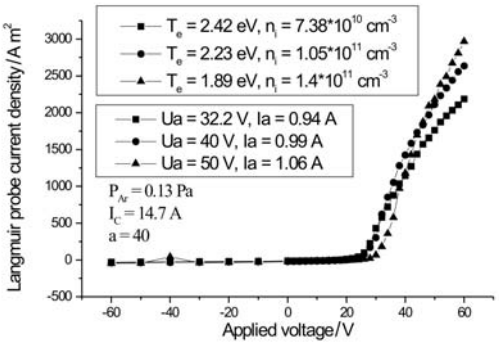

Fig. 11 Plasma potential influence on the plane plasma parameters

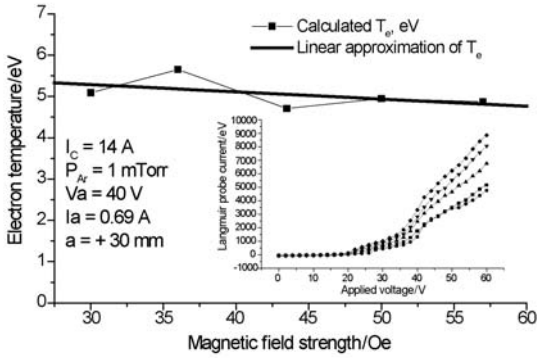

Fig. 12 External magnetic field influence on the electron temperature

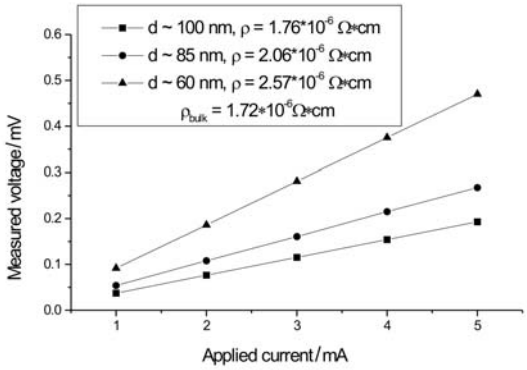

Fig. 13 Four-point probe measurement of the Cu films

Figure 12 presents the external magnetic field influence on the electron temperature. The experimental probe characteristics measured for different magnetic field strength are shown in the including. The electron temperature slightly depends on the magnetic field and decreases at about 5% for twice an increase in the magnetic field

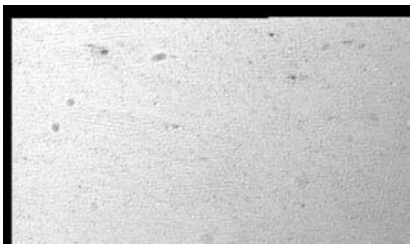

Fig. 14 Microscope photography (x800) of the Cu coating (1 cm is 12.5 μm)

strength. This influence is defined by the ion concentration increase with the magnetic field, owing to the electron confinement improvement.

Triode sputtering systems with plane plasma discharge was tested using Cu targets. Sputtering voltage was ~1500 V and ion target current was ~10 mA. Figure 13 presents a sheet resistance measurement. As shown there, the four-point probe measurement is quite linear. Therefore, the conductive mechanism is probably metallic. Resistivity of deposited films increases with the thickness increase and tends to a limit, which relates to the bulk resistivity. As appears in Fig. 14, the Cu coating looks smooth and homogeneous along the substrate surface.

Conclusions

A detailed investigation of an artificial plane plasma discharge, with a relatively low pressure, is presented in the work. The basic plasma parameters: electron temperature and charge carriers concentration, were calculated from the experimentally measured Langmuir probe I–V characteristics. Calculations were based on the collision-less model of a thin layer of volume charge, surrounding the small probe. The obtained plasma discharge appears as a plane wall with a defined thickness that is lower than the mean free path of atoms in the vacuum chamber. This plane plasma phenomenon enables sputtering of various materials without collisions between the sputtered atoms and the plasma ions. The measured temperature of the probe, placed within the plasma has not exceeded 140°C. Hence, substrate temperature may be used as an independent parameter of the deposition process.

Cu sputtering using this plane plasma was tested. The obtained films had a metallic type of conductivity and their resistivity was influenced by the film thickness.

References

1 W. N. G. Hitchon, Plasma processes for semiconductor fabrication, Cambridge University Press, N.Y. 1999.
2 M. A. Lieberman and A. J. Lichtenberg, 'Principles of plasma discharges and materials processing', Wiley, N.Y. 1994.
3 T. Mousel, W. Eckstein and H. Gnaser, Nucl. Instr. Meth., B 152 (1999) 36.

4 'Plasma Damage', http://www.timedomaincvd.com/CVD Fundamentals/plasmas/plasma_damage.html
5 B.V. Alekseev and B. A. Kotelnikov, 'Plasma diagnosis by the probe method', Energoatomizdat, Moscow (Russian), 1988.
6 G. Golan, A. Axelevitch, R. Margolin and E. Rabinovitch, Microelectronics Journal, 32 (2001) 60.
7 R. H. Huddlestone and S. L. Leonard, 'Plasma Diagnostic Techniques', Academic Press, N.Y. 1965.
8 F. Mulally, 'Plasma Probe Investigation', December 2000, http://www.netsoc.ucd.ie/~fergalm/plasma/plasma.html
9 L. I. Maissel and R. Glang, 'Handbook of Thin Film Technology', McGraw-Hill, N.Y. 1970.
10 Course of 'Semiconductors', University of Kiel, Faculty of Engineering, http://www.techfak.uni-kiel.de/matwis/amat/semi_en
11 A. Möller, 'Probe Measurements of Fluctuations and Transport in Reversed-Field Pinches', Dissertation thesis, Royal Institute of Technology, Stockholm 1998.
12 R. J. Stokes and D. F. Evans, 'Fundamentals of Interfacial Engineering', Wiley, N.Y. 1997.
13 R. Kossowsky, 'Surface Modification Engineering', CRC Press, Boca Raton, 1989.
14 J. D. Huba, 'Plasma Formulary', Naval Research Laboratory, 2000.
15 'Ion Flux to Surfaces: the Bohm Velocity', http:_//www.timedomaincvd.com/CVD_Fundamentals/plasmas/ion_flux.html